Revista Mexicana de Astronomía y Astrofísica Serie de Conferencias (RMxAC), **56**, 45–47 (2024)

https://doi.org/10.22201/ia.14052059p.2024.56.05

STUDY OF DIFFUSE SOURCES ON THE RADIOHALO OF TXS 0828+193

M. M. Moyano[1]

RESUMEN

En este trabajo analizamos imágenes del Telescopio Espacial Hubble de TXS 0828+193, una radiogalaxia con alto corrimiento al rojo (z=2.572), con el objetivo de estudiar un par de débiles y difusas fuentes descubiertas recientemente, para confirmar fotométricamente su relación física con esta radiogalaxia. Mediante el uso combinado de SExtractor y GAIA se obtuvieron valores de $m_{\rm AB} \approx 26$ y $m_{\rm AB} \approx 27.5$, respectivamente para ambas regiones. Aunque estos valores son muy débiles para poder obtener fotométricamente el corrimiento al rojo correspondiente, presentamos algunas propuestas que permiten determinar la naturaleza de estas dos regiones difusas.

ABSTRACT

In this work, images from the Hubble Space Telescope of TXS 0828+193, a radio galaxy at high redshift (z=2.572), were analized with the aim of studying two recently detected diffuse sources towards it and try to photometrically confirm its physical relationship with it. By means of the combined use of the softwares SExtractor and GAIA, there were obtained values of $m_{\rm AB} \approx 26$ and $m_{\rm AB} \approx 27.5$ for both regions respectively. Although these values are weak to be able to obtain the corresponding redshift photometric data, we present some possible astrophysical scenarios that could help to discern the nature of these two diffuse regions.

Key Words: galaxies: high redshift — radio lines: galaxies — galaxies: halos

1. INTRODUCTION

TXS 0828+193 is a high redshift radio galaxy contained in the TEXAS catalogue. This catalog was created from the Texas Survey, a survey of radio sources discrete tests with $\delta \in [-35.5°, +71.5°]$ (B1950), at the frequency of 365 MHz ($\lambda = 82$ cm) using the Texas Interferometer of the Radio Astronomy Observatory of the University of Texas (UTRAO) during the years 1974 to 1983 (Douglas et al. 1996). The source is embedded in an extensive Lyman α nebula and is associated with a radio source with a flux of 22 mJy at around 4.7 GHz. Its structure consists of various components and includes two jets sensed to the frequency of the survey, one of them extending from the core. On the other hand, its optical structure has various components grouped in a triangular shape, with a double bubble at one end (Morais et al. 2017). These authors also propose that TXS 0828+193 would be surrounded by a bubble of expanding gas, with a radius of ≈ 16 Kpc (2 arcsec), within which the kinematically closest gas would be found disturbed. They also assume a rate of expansion of ≈ 1000 km s^{-1} and find it plausible that the radio broadcast has started simultaneously with bubble expansion. Using the IRAM Plateau de Bure interferometer, Nesvadba et al. (2009) detect an intense line of emission of CO(3-2) in the halo of TXS 0828+193, at a distance of ≈ 10 arcsec southwest of the geometric center of the radio galaxy. The photometric counterpart from ultraviolet to infrared could not be detected, which implies that it would have a low stellar mass and little star formation rate. That is why I propose that the line would be emitted by a rotating satellite galaxy, or by two satellite galaxies of the halo of TXS 0828+193, a few kpc away from it. They also suggested that this line originates from clouds or filaments of the same halo. This work was devoted to analyzing images of the Hubble Space Telescope (HST) of this radio galaxy. They would reveal what might be the optical counterpart of the emission line detected by Nesvadba et al. (2009). With this we could determine what is its origin and would make it possible to discern whether there is a physical relationship between them.

[1]Observatorio Astronómico de Córdoba, Universidad Nacional de Córdoba, Argentina, Laprida 854, Córdoba, Córdoba, Argentina (martin.manuel.moyano@mi.unc.edu.ar).

2. CO(3-2) EMISSION LINE

The CO(3-2) emission line identified by Nesvadba et al. (2009) is aligned with the axis of the radio jet and consists of two compact components, which were identified as SW1 and SW2 respectively. At the spatial resolution of their observations, these two components have the same position, but different blueshifts, ΔV(SW1)= -200 km s^{-1} and

IAR's 60th anniversary: Prospects for low-frequency radio astronomy in South America (November 15-18, 2022)
Editors: Paula Benaglia and Ileana Andruchow - DOI: https://doi.org/10.22201/ia.14052059p.2024.56.05

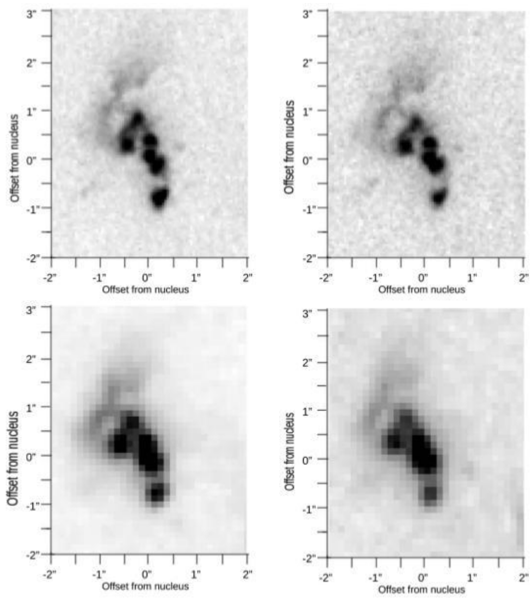

Fig. 1. Images of TXS 0828+193 obtained with the WFC3 and ACS cameras of the HST, taken from Morais et al. (2017). The upper panels show, from left to right, the radio galaxy in the F606W and F814W filters, while the lower panels show the radio galaxy in the F110W and F160W filters. In all of them, north is oriented towards up and east to the left.

ΔV(SW2)= -900 km s^{-1} with respect to the radio galaxy. In addition to being blueshifted, SW1 and SW2 are also on the side of the radio galaxy in which the diffuse Lyman-α halo is blueshifted (Nesvadba et al. 2009). These authors had previously estimated the systemic velocity from the framework of the optical reference of integral field spectroscopy performed in TXS 0828+193 (Nesvadba et al. 2008).

3. HST PHOTOMETRIC IMAGES

Four photometric images of the radio galaxy TXS 0828+193 were used to develop this work. These were taken from the HST database and published by Morais et al. (2017) (2017), and are shown in Figure 1. Two of them were acquired using the WFC3 camera filters F110W and F160W and the other two were acquired with the ACS camera filters F814W and F606W. It is important to mention that the WFC3 camera has a resolution of $0.13''$px^{-1}, while that of the camera ACS is $0.049''$px^{-1} (see Tables 1 and 2).

4. RESULTS

From the analysis performed on the HST images, we identified nebulous objects at an angular distance of $\approx 10''$ from the geometric center of the radio galaxy, whose positions appear to match the sources associated with the emission of the CO(3-2)

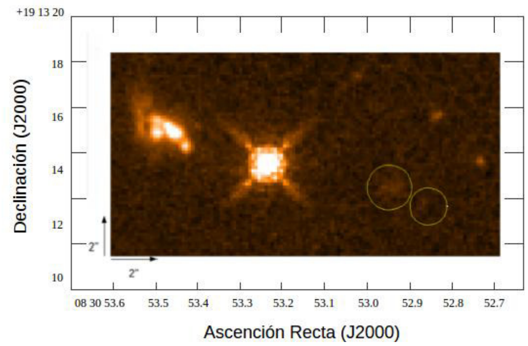

Fig. 2. HST image taken with the F160W filter of the radio galaxy. The two nebulosities analyzed are contained in the yellow circles. Again, north is up and east is left.

line mentioned in the work of Nesvadba et al. (2009). In Figure 2 their positions are indicated with yellow on the image taken with the F160W filter.

In each of the four analyzed images the signal-to-noise (S/N) ratio was measured using the SEXtractor software. To do this, we firstly determined the standard deviation of the sky background; then the ratio (S/N) of each pixel of the image was defined as the difference between the pixel flux and the flux average of the sky background (surrounding pixels), expressed in standard deviations of the sky background. In this procedure, we considered a detection if the set of adjacent pixels, with ratio $(S/N) > 3$, covered an area greater than 0.03 arcsec^2. Once one of the objects was detected on an image, we measured the signal to noise ratio and the magnitude in the rest of the images, considering the same position.

In the images corresponding to the WFC3 camera we measure the magnitudes using the software SExtractor. On the other hand, in the corresponding image to the F606W filter it was only possible to distinguish one of the two nebulosities, which magnitude was also measured using, separately, the softwares SExtractor and GAIA. Tables 1 and 2 show the results of these measurements. In the first columns of them are detailed the acquisition dates and in the second the filters used to obtain every image are mentioned; from the third to the fifth columns are consigned, respectively, the effective wavelength of the filter, the range of wavelengths covered by it and this range measured in the laboratory reference system. In the sixth and seventh columns there are listed the coordinates of the nebulous objects, which coincide with those of the line of CO(3-2) emission identified by Nesvadba et al. (2009); the eighth column shows the ratio (S/N) measured with SExtractor, while the latter provides the magnitudes obtained in the AB photometric system (Oke 1974;

IAR's 60th anniversary: Prospects for low-frequency radio astronomy in South America (November 15-18, 2022)
Editors: Paula Benaglia and Ileana Andruchow - DOI: https://doi.org/10.22201/ia.14052059p.2024.56.05

TABLE 1

RATIOS (S/N) AND MAGNITUDES DETERMINED ON THE HST IMAGES CORRESPONDING TO THE NORTHERNMOST NEBULOUS OBJECT OF THE PAIR (ON THE LEFT IN THE FIGURE 2).

Date	Filter	λ_{ef} [Å]	λ_{obs} range [Å]	λ_0 range [Å]	α	δ	S/N	$m_{\rm AB}$
2010/03/10	F110W	11534	9319-13749	2608.903849.10	127.720803	19.2193589	2	26.4 ± 0.2
2011/05/08	F160W	15369	14027-16710	3927.074678.19	127.720725	19.2193233	3	25.4 ± 0.2
2010/03/26	F814W	-	6885-8000	1927.492463.61	-	-	-	-
2010/03/28	F606W	5808	4633-7180	1297.032010.08	-	-	-	-

TABLE 2

RATIOS (S/N) AND MAGNITUDES DETERMINED ON THE HST IMAGES CORRESPONDING TO THE SOUTHERNMOST NEBULOUS OBJECT OF THE PAIR (ON THE RIGHT IN THE FIGURE 2).

Date	Filter	λ_{ef} [Å]	λ_{obs} range [Å]	λ_0 range [Å]	α	δ	S/N	$m_{\rm AB}$
2010/03/10	F110W	11534	9319-13749	2608.903849.10	127.720492	19.2189763	2	27.3 ± 0.3
2011/05/08	F160W	15369	14027-16710	3927.074678.19	127.720514	19.2189670	2	27.0 ± 0.4
2010/03/26	F814W	-	6885-8000	1927.492463.61	-	-	-	-
2010/03/28	F606W	5808	4633-7180	1297.032010.08	127.720499	19.2189704	3	28.4 ± 0.4

Oke & Gunn 1983).

4.1. *Conclusions*

In this work, four HST archival images of the radio galaxy TXS0828+193 were used in order to obtain the integrated magnitudes $m_{\rm AB}$ of two diffuse regions identified around it, which could be the photometric counterpart of the CO(3-2) line detected by Nesvadba et al. (2009). As can be seen from Tables 1 and 2, very weak magnitudes and low signal on noise ratios (S/N) were obtained (≈2–3), which prevents obtaining the photometric redshift of these regions. Therefore, it will be necessary to perform spectroscopic observations of better spatial resolution to determine these redshifts and to be able to confirm whether or not they are associated with the CO(3-2) emitting sources, as suggested by Nesvadba et al. (2009).

Under these conditions, it would be difficult to obtain useful spectra from the optical to the far infrared range, even with telescopes like GEMINI, since the magnitudes obtained in the four analyzed HST images were very high. In fact, for this radio galaxy spectroscopic simulations were performed with GEMINI GMOS-IFU and gave a signal on noise ratio (S/N)$<\sim$7 for 20 exposures of 15 minutes each ($FWHM = 1''$). A superior alternative would be to observe them on radio with some instrument that enables a spatial resolution of $0.5''$. Analyzing the features offered by the radio astronomical observatory Karl G. Jansky Very Large Array (VLA), it turns out that its A configuration achieves this resolution at 4 GHz.

Another possibility to take into account in the interpretation of these detected nebulosities, would be to consider that they indicate star formation activity associated with molecular gas. According to the values of Table 2, SW2 would not appear to be reddened enough (A. Humphrey 2018, private communication).

Regarding the emission lines, another aspect to take into account of the photometric filters available at the HST measurements is that many of the brighter emission lines that characterize these types of objects lie outside their spectral ranges. For example, z=2.57: $Ly_\alpha\sim$4340 Å, [O III]5007$\sim$17880 Å, $H_\alpha\sim$23430 Å, among others. However, at this edshift the line [O III]3727 would be at $\sim$23430 Å and therefore could be detected in the range covered by the F110W filter, but probably most of the flow measured in this band would be dominated by continuous emission and not by this emission line.

REFERENCES

Douglas, J. N., Bash, F. N., Bozyan, F. A. et al. 1996, AJ, 111, 1945
Morais, S. G., Humphrey, A., Villar-Martin, M., et al. 2017, MNRAS, 465, 2698
Nesvadba, N. P. H., Lehnert, M. D., Frye, B., et al. 2008, A&A, 491, 407
Nesvadba, N. P. H., Neri, R., De Breuck, C., et al. 2009, MNRAS, 395, 16
Oke, J. B. 1974, ApJS, 27, 210
Oke, J. B. & Gunn, J. E. 1983, ApJ, 266, 713